

CO₂ Selective, Zeolitic Imidazolate Framework-7 Based Polymer Composite Mixed-Matrix Membranes

Tina Chakrabarty¹, Pradeep Neelakanda¹ & Klaus-Viktor Peinemann¹

¹ Advanced Membrane and Porous Materials Center, King Abdullah University of Science and Technology (KAUST), 23955-6900, Thuwal, Saudi Arabia

Correspondence: Tina Chakrabarty, Advanced Membrane and Porous Materials Center, King Abdullah University of Science and Technology (KAUST), 23955-6900, Thuwal, Saudi Arabia. E-mail: tina.chakrabarty@kaust.edu.sa

Received: February 27, 2017

Accepted: March 22, 2017

Online Published: May 17, 2018

doi: 10.5539/jmsr.v7n3p1

URL: <https://doi.org/10.5539/jmsr.v7n3p1>

Abstract

CO₂ removal is necessary to mitigate the effects of global warming but it is a challenging process to separate CO₂ from natural gas, biogas, and other gas streams. Development of hybrid membranes by use of polymers and metal-organic framework (MOF) particles is a viable option to overcome this challenge. A ZIF-7 nano-filler that was synthesized in our lab was embedded into a designed polymer matrix at various loadings and the performance of the mixed matrix membranes was evaluated in terms of gas permeance and selectivity. Hybrid membranes with various loadings (20, 30 and 40 wt%) were developed and tested at room temperature by a custom made time lag equipment and a jump in selectivity was observed when compared with the pristine polymer. A commercially attractive region for the selectivity CO₂ over CH₄ was achieved with a selectivity of 39 for 40 wt% particle loading. An increase in selectivity was observed with the increase of ZIF-7 loadings. Best performance was seen at 40% ZIF-7 loaded membrane with an ideal selectivity of 39 for CO₂ over CH₄. The obtained selectivity was 105% higher for CO₂ over CH₄ than the selectivity of the pristine polymer with a slight decrease in permeance. Morphological characterization of such developed membranes showed an excellent compatibility between the polymer and particle adhesion.

Keywords: Carbon dioxide separation, mixed-matrix membranes, nanomaterials, zeolitic imidazolate frameworks, ZIF-7 fillers; gas separation

1. Introduction

Natural gas is a paramount energy source of the future and the most environmental friendly non-renewable fossil fuel until now. The composition of natural gas-widely depends on the reservoir source but mainly composes of methane (30-90%), ethane, propane, carbon dioxide (CO₂), nitrogen (N₂) including smaller traces of hydrogen sulphide (H₂S), helium (He), and water vapour as impurities (Baker and Lokhandwala, 2008). It is essential to remove CO₂ from natural gas before processing due to the formation of carbonic acid by the reaction of CO₂ with water vapor which corrodes the gas transport pipelines (Bhide and Stern, 1993). Presence of CO₂ decreases the heat capacity of natural gas and the concentration of CO₂ over 2 mole% makes the gas transport less viable (Baker, 2001).

Membrane technology receives a significant attention for the separation of CO₂ from natural gas (Adeole et al., 2013) and it competes with conventional technologies like amine scrubbing (Bottoms, 1930) and cryogenic distillation process (Michael et al., 2011). Polymeric membranes are widely used in the membrane-based gas separation process due to their ease of fabrication, low operation cost, and high energy efficiency. Membranes for natural gas processing from cellulose acetate polymer were first commercialized during the 1980s for CO₂ removal (Schell, 1989) but in general polymeric membranes are prone to a trade-off between permeability and selectivity (Robeson, 2008), which means that membranes with high permeance have a low selectivity and vice versa. One of the approaches to overcome such limitation is the incorporation of selective fillers namely metal-organic frameworks (MOF), carbon nanotubes and others into the polymer matrix to develop mixed matrix membranes (MMM) (Rodenas et al., 2015; Li & Peinemann, 2013; Ahmed et al., 2014). Filler properties such as size, chemical structure, and porosity are some of the parameters to be considered for selection. Compatibility between polymer and filler is one of the important parameters for a defect-free membrane fabrication. Proper selection of materials in MMM combines the merits of both filler and polymer to achieve a high gas selectivity and maintain permeability.

One of the widely used filler material in MMM for CO₂ separation is the zeolitic imidazolate framework ZIF-7. ZIFs are a sub-class of metal-organic frameworks (MOF) (Song et al., 2012; Bae et al., 2010; Dai et al., 2012). Xiaochun, Jiepeng, and Xiaoming (2003) discovered ZIF-7 by bridging imidazolate (benzimidazole) linker with a transition metal cluster (Zn²⁺) to form a 3D structure with sodalite (SOD) framework topology. ZIF-7 is a six-membered structure with a pore size of 0.3 nm (Bergh et al., 2011), it is hydrophobic in nature. It exhibits excellent chemical and thermal stability (Park et al., 2006) and is stable up to 500°C (Li et al., 2010). In this work, ZIF-7 has been used as a filler material with a CO₂-philic co-polymer polyacrylonitrile-*r*-poly (ethylene glycol) methyl ether methacrylate (PAN-*r*-PEGMA) synthesized in our laboratory (Karunakaran et al., 2017) for the development of mixed matrix membranes.

MMMs with various ZIF-7 loadings (20, 30 and 40%) to the weight of the polymer was developed and their permeation properties were evaluated with single gases of CO₂ and CH₄ permeation on a custom made time lab equipment (Karunakaran et al., 2017). Polyester backed ultrafiltration range polyacrylonitrile (PAN) polymeric membrane was used as a mechanical support for the membranes developed in this work.

2. Experiments

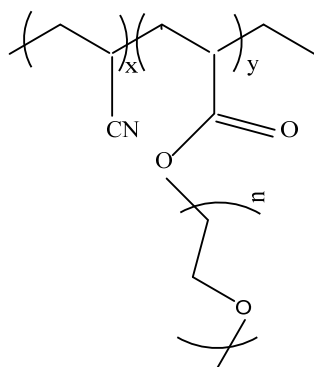
2.1 Materials and Methods

Commercially available PAN membrane support was kindly provided by GMT Membrantechnik GmbH (Rheinfelden) Germany. Zinc nitrate hexahydrate (Zn(NO₃)₂·6H₂O, 99%), benzimidazole (bIm, >98%) were purchased from Sigma-Aldrich and Across-organics respectively. Dimethylformamide (DMF), tetrahydrofuran (THF) and methanol solvents were purchased from Sigma-Aldrich and Fisher Scientific respectively. Solvents were used as received without any additional purification. Pure gases of CO₂ and CH₄ (purity 99.995%) were purchased from Air liquid Alkhafrah Industrial gases, Saudi Arabia.

2.2 Synthesis of ZIF-7 and PAN-*r*-PEGMA67 Polymer

ZIF-7 particles were synthesized following the procedure reported by Wang et al., 2016. Zn(NO₃)₂·6H₂O of 6.8 gm was dissolved in 250 ml of DMF and benzimidazole of 6 gm was dissolved in 250 ml of methanol at room temperature individually. Previously dissolved metal and ligand solutions were mixed and stirred together for 6 hours to get a white suspension. The final product of ZIF-7 was obtained by centrifuging and rinsing the white suspension three times with methanol to remove any excess solvents. The ZIF-7 particles were oven dried at 60°C for 12 hours under vacuum.

Many polymers have been reported for the separation of CO₂. An attractive polymer group for this separation is polyether based polymers, which show high CO₂ selectivities due to the affinity of PEG or PEO with CO₂. By blending PEG with Pebax 1657 polymer Car, A., Stropnik, C., Yave, W., and Peinemann K. V. (2008) reported an enhancement in the gas transport performance. In this work, we have used a laboratory synthesized CO₂-philic polymer PAN-PEGMA67 which has a high content of PEGMA (950Da) (Karunakaran et al. (2017), scheme 1 shows the structure of the polymer. For the following reasons we chose this polymer to achieve a better gas separation property: (1) Due to the higher presence of PEG units in the polymer, it has higher selectivity of CO₂/CH₄ when compared with the commercial Pebax1657 (2) the polymer dissolves well in a mixture of ethanol/water (70/30 wt%) which is an environmental-friendly binary mixture for membrane preparation (3) a commercial PAN membrane was used as a porous support material for all the membranes developed in this work. Since PAN-*r*-PEGMA67 contains PAN as a copolymer we expect a good adhesion between the support and the coating for a better gas separation performance



Scheme 1. Structure of PAN-*r*-PEGMA67 co-polymer

2.3 Membrane Preparation

PAN-*r*-PEGMA67 polymer (2wt %) was dissolved in a mixture of ethanol and water by (70:30)wt % at 75°C temperature for 4 hours under stirring. The polymer solution was filtered by a steel filter of 32µm pore size to remove any dust and gel particles. The synthesized ZIF-7 particles were dispersed into the polymer solution with different particle loadings. The mixture was sonicated and stirred for 12 hours at room temperature for a complete dispersion.

Particle loadings were calculated as:

$$\text{Particle loading} = \frac{\text{Weight of particles}}{(\text{Weight of particles} + \text{Weight of polymer})} \times 100 \text{ wt\%} \quad (1)$$

The PAN support membrane was placed between a square-shaped Teflon plate and a frame set-up with silicone rubber gasket. These are stacked and held tightly by binder clips to avoid any leak. A known volume of the dispersed mixture was poured into the plate and frame set-up and was allowed to dry at room temperature for 24 hours. Dried membranes were carefully removed from the set-up and further dried in an oven at 60°C for 12 hours under vacuum. Mixed matrix membranes with various ZIF-7 loadings (0, 20, 30 and 40%) with respect to the polymer weight were correspondingly denoted as MMM0, MMM20, MMM30 and MMM40 in this article. Membranes developed with 50% loadings were brittle in nature and their gas permeation was not evaluated due to its difficulty in handling.

2.4 Characterization

X-ray diffraction measurement (XRD) for the developed samples were carried out in reflection mode with a Bruker D8 Advanced XRD instrument equipped with CuK-alpha (1.54 Å wavelength, λ) with LynxEye 1-d as a detector. Data were collected by step-scan mode in the range of 0.02-degree step size with an interval of 2 sec.

Dense films were made from pristine PAN-*r*-PEGMA67, MMM20, MMM30 and MMM40 for ATR-FTIR measurements. Spectra of the dense membranes were recorded using Nicolet iS10 (Thermo Scientific) FTIR spectrometer. Data were collected for 16 scans at ambient temperature with a resolution of 4 cm⁻¹.

Thermal stability of ZIF-7, pristine polymer and MMM samples were measured by a thermogravimetric analyzer (NETZSCH, TG209F1 Iris). Samples were conditioned at 80°C under vacuum before analysis to remove any guest molecules from the pores. All the experiments were carried out at a heating rate of 20 °C/min from room temperature to 1000 °C under a nitrogen atmosphere.

Scanning electron microscopy (SEM) images were performed on a Magellan 400 SEM, FEI/ Thermo scientific equipped with field emission gun with the unicolor mode. A through the lens detector (TLD) and concentric backscatter detector (CBS) were used for surface and cross-sectional imaging. Samples were fractured in liquid nitrogen for the cross-sectional imaging and were sputter-coated to a thickness of 3 nm with iridium to avoid any charging effect. Atomic Force Microscopy (AFM) analysis was performed using an Agilent (Model 5400) microscope for all the samples in this work. Images of 2D and 3D views were taken by tapping mode to avoid any damage to the AFM tip which has a resonant frequency of 60-80 Hz and a spring constant of 3Nm⁻¹. A transmission electron microscopy (TEM) FEI-Tecnaï twin equipped with ORIUS SC1000 camera (Gatan) at 120 kV was used to analyze the ZIF-7 particles shape and size.

2.5 Gas Permeation Test

Gas permeation experiments were determined with a constant volume / variable pressure set up at 25°C temperature and 600 mbar as feed pressure for the measured gases. Membrane permeance was calculated by using the following equation:

$$J = \frac{V \times 22.4}{R \times A \times T \times t_s} \ln \left(\frac{p_F - p_0}{p_F - p_{p(t)}} \right) \quad (2)$$

where V is the downstream volume (m³), R is the ideal gas constant (0.083 L atm K⁻¹ mol⁻¹), T is the permeation temperature (K), A is the membrane area (m²), t is the time (s), P_F and P₀ are the pressure at feed side (bar) and P_{p(t)} is permeate pressure.

3. Results and Discussion

3.1 Characterization of ZIF-7 filler and PAN-*r*-PEGMA67 MMMs

Figure 1 illustrates the XRD patterns of pure ZIF-7 particle and pristine PAN-*r*-PEGMA67 polymer.

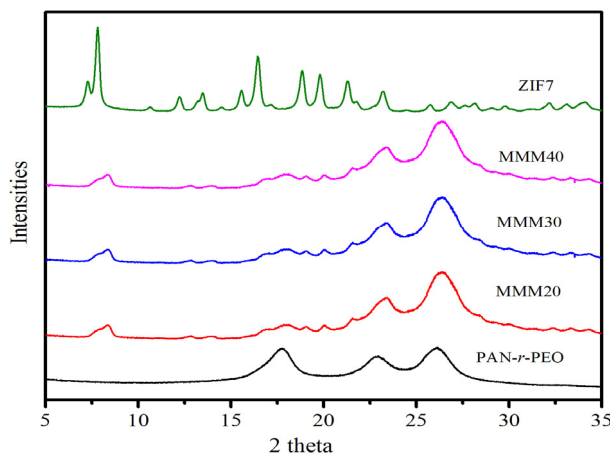


Figure 1. XRD spectra for ZIF7, PAN-*r*-PEGMA67, MMM20, MMM30, and MMM40

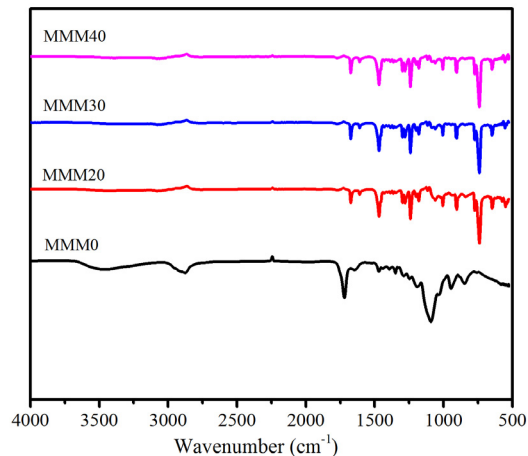


Figure 2. FTIR spectra for MMM0, MMM20, MMM30 and MMM40 membranes

The wide-angle XRD (WXRD) has a broad 2θ peak observed near 18° but due to the amorphous nature of the polymer, no sharp peaks were detected. The structural data of synthesized pure ZIF-7 by powder X-ray diffraction (PXRD) was in good agreement with the reported values (Maythalyon et al., 2017; Kang et al., 2013). In Figure 1 the angles of diffracted peaks of the samples MMM-20, 30 and 40 series were shifted to broader angles when compared with virgin ZIF-7 particles. These angle changes correspond to the change of d-spacing in ZIF-7 particles due to their interaction with the polymer.

FTIR (Figure S1) peaks that appeared at 1455 and 777 cm^{-1} on pure ZIF-7 particle were identified as C=C and C-H bonds which resulted from benzene functional group present in benzimidazole. Figure 2 shows the FTIR spectra of mixed matrix membranes MMM-20, 30 and 40.

Existence of peaks at 1455 cm^{-1} and 777 cm^{-1} and the couplet of different peaks in the range of 1200 - 1800 cm^{-1} and at 700 cm^{-1} confirm the presence of ZIF-7 and were in good agreement with the literature reports (Tu et al., 2014; Maythalyon et al., 2017; Kang et al., 2013)

3.2 Thermal Properties of ZIF-7 Composite Mixed-Matrix Membranes (MMMs)

Figure 3 and Figure 4 show the thermogravimetric analysis (TGA) curves of pure ZIF-7 particles, pristine PAN-*r*-PEGMA67 polymer and MMM-20, 30 and 40 % particle loaded samples. In Figure 3 a two-step weight loss was observed, an initial and final weight loss of 13.1% and 62.5% at 250°C and 500 - 600°C respectively. Initial weight loss was due to the evaporation of DMF solvent present in ZIF-7 cages and the final weight loss was due to the decomposition of ZIF-7 to zinc oxide. TGA curves obtained in this work matches well with the earlier reports (Kang et al., 2013).

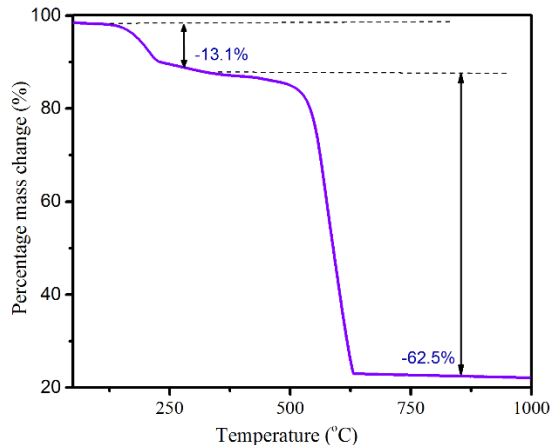


Figure 3. TGA weight loss curve for ZIF-7 particles

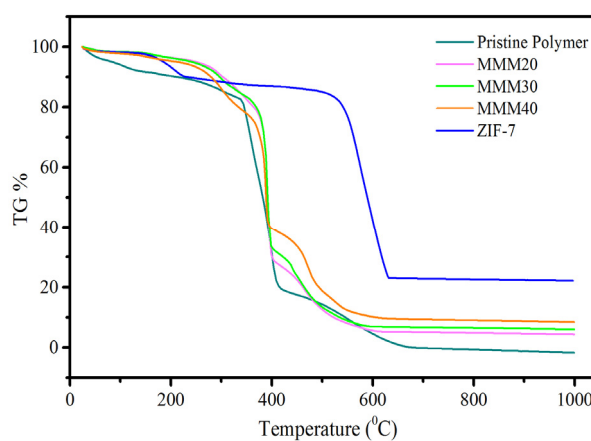


Figure 4. TGA curve of ZIF-7, pristine polymer and MMM20, MMM30 and MMM40

In Figure 4 an initial weight loss in pristine polymer occurred around 150°C due to the presence of moisture content. Compared with the pristine polymeric membrane (MMM0), the thermal stability of MMM improved after the incorporation of ZIF-7 with an increased 1st and 2nd degradation temperatures from 320°C to 380°C and 400 to 450°C. Table 2 shows that the final residue of ZnO increases along with the increase of ZIF-7 loadings in the MMM. However, such residual values of MMM were less when compared with the final residue of pure ZIF-7 particles.

3.3 Morphology of ZIF-7/MMMs

The surface morphology of as-prepared ZIF-7 particles were analyzed by FE-SEM (Figure 5a) and the approximate size of the particles was in the range of 40-50 nm. As shown in Figure 5b, particle shape and size were re-confirmed with TEM analysis.

Figure 6 and Figure 7 depicts the SEM images of surface and cross-section of pristine and ZIF-7 loaded MMM respectively. Surface images of various ZIF-7 loaded membranes shows a good distribution of particles with no agglomeration (Figure 6b-6d) which helps to improve the membranes gas separation property with no defect formation.

Table 1. Thickness measurement of membrane selective layer from SEM cross-section

Membranes	Thickness (μm) measured from SEM Cross-section			Average thickness (μm)
MMM0	1.5	1.7	1.1	1.5
MMM20	1.6	1.7	2.1	1.9
MMM30	3.3	3.5	3.7	3.5
MMM40	7.3	7.1	7.5	7.3

A detailed AFM height profile for the developed MMMs is given in Figure S2. The surface of the neat membrane was found to be smooth but an incremental increase of roughness was observed with the increase of particle loadings on (Figure 8b-8d). The thickness of the selective layer for all MMMs was analyzed by SEM cross-section (Figure 7a-7d) at least at three different locations of each sample and the average thickness value is shown in Table 1. SEM cross-section images confirm that the membrane thickness increases with the higher filler loadings for the MMM samples.

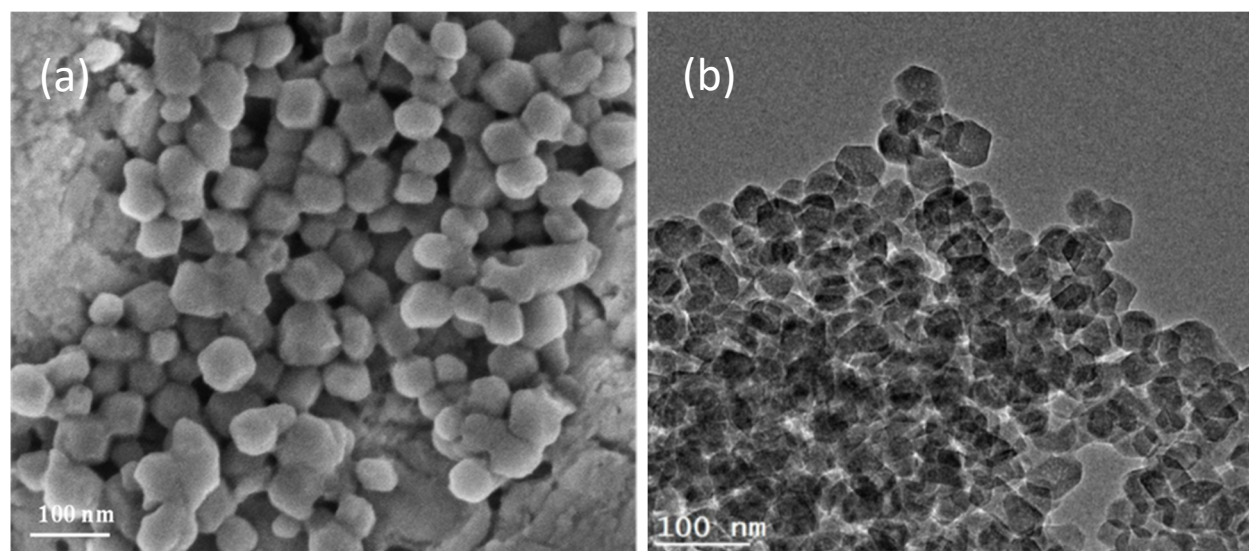


Figure 5. (a) FESEM images of as-synthesized ZIF-7 (b) TEM images of ZIF-7

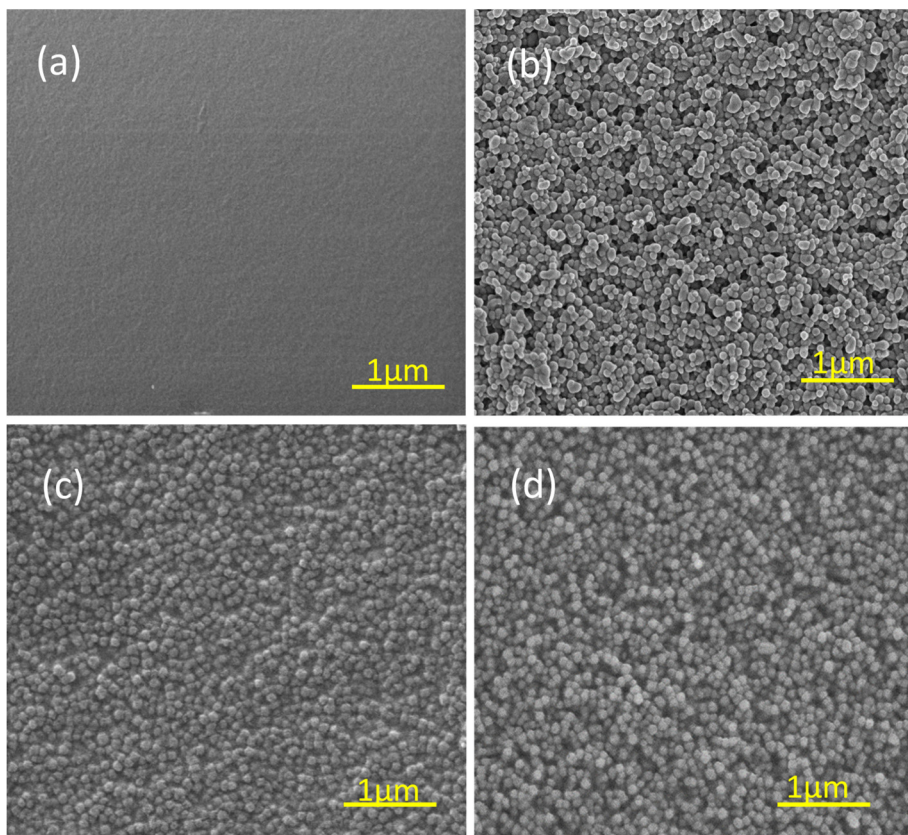


Figure 6. SEM images of composite membrane top view (a) MMM0 (b) MMM20 (c) MMM30 and (d) MMM40

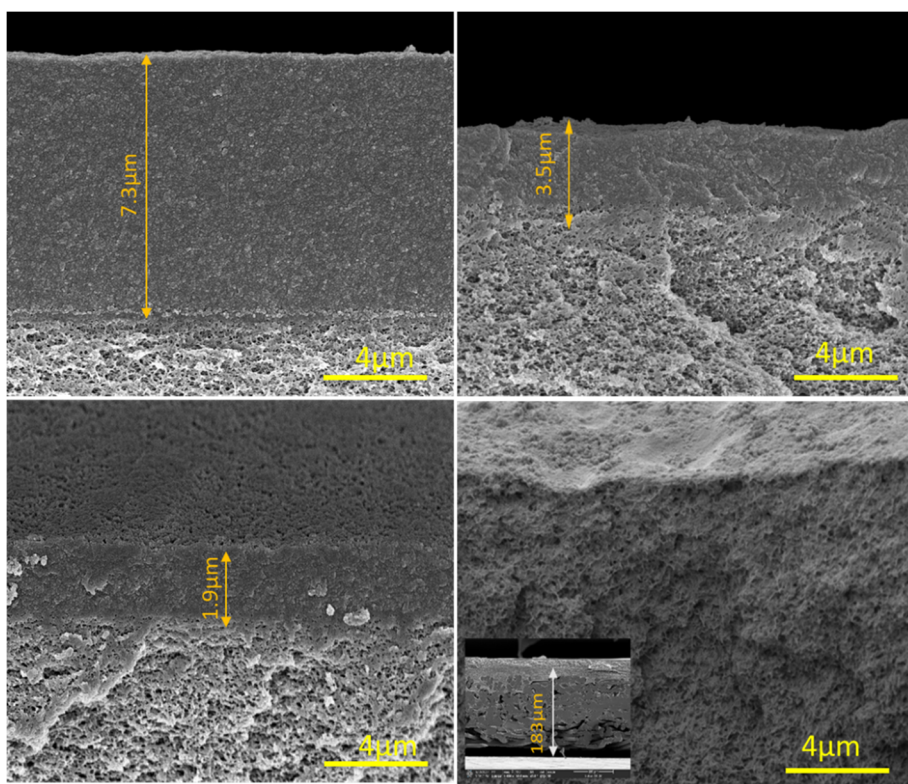


Figure 7. Cross-sectional SEM images for (a) MMM40 (b) MMM30 (c) MMM20 and (d) MMM0, PAN support (inset picture)

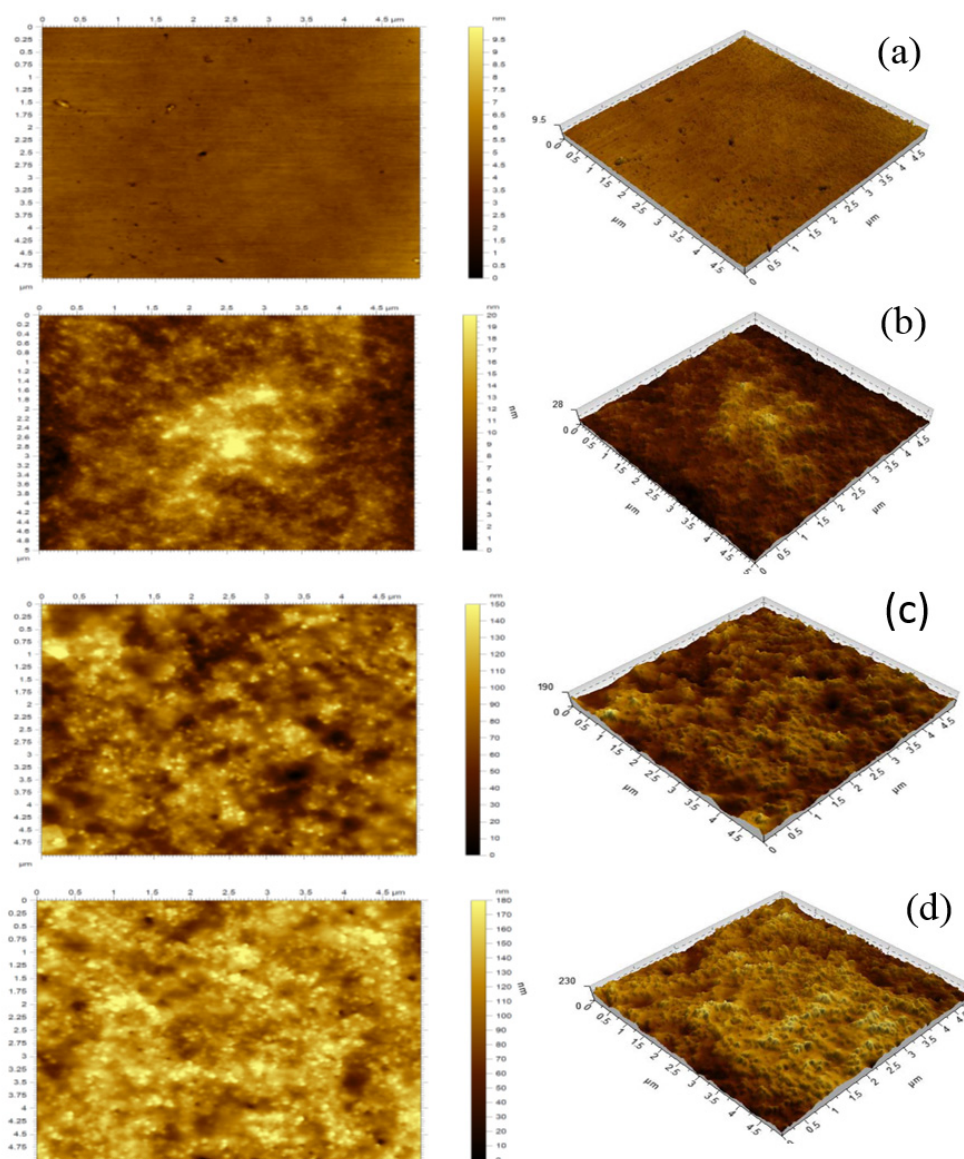


Figure 8. 2D (left) scale $5\mu\text{m}$ and 3D (Right) topography of (a) MMM0 (b) MMM20 (c) MMM30 and (d) MMM40 membranes

3.4 ZIF-7 Loading in Mixed-Matrix Membranes

The determination of accurate particle loading is important to estimate the performance of MMM. In this work, thermogravimetric analysis (TGA) was used to determine the loading percentage of ZIF-7 particles in the MMMs (Zhang et al., 2012). Samples to be tested were annealed until $200\text{ }^{\circ}\text{C}$ in air for 5 h to remove any guest molecules present in the sample. Subsequently, the temperature was increased to $1000\text{ }^{\circ}\text{C}$ with a heating rate of $10\text{ }^{\circ}\text{C}/\text{min}$ in air. At $550\text{ }^{\circ}\text{C}$ both the polymer and ZIF-7 particles got decomposed and oxidized leaving zinc oxide as residue. Percentage loading of ZIF-7 from the residue in mixed-matrix membranes was then back-calculated on Table 2.

Table 2. TGA analysis results of residue and calculated loading of ZIF-7

Loadings (wt %)	ZIF-7	MMM20	MMM30	MMM40
ZnO	31	6.0	7.2	10.4
Zn	25	4.8	5.7	8.3
ZIF-7	N/A	19.5	23.1	33.4

Calculated loading of ZIF-7 in wt% and the TGA determined zinc mass percentage for each type of mixed-matrix membrane are shown in Table 2. The zinc mass percentage determined by TGA was 25% and the theoretical mass percentage by their molar mass value was calculated as 35%. From the obtained residual values, higher particle loadings had an increased presence of zinc which helps to determine the percentage loading of MMMs theoretically.

3.5 Pure Gas Permeation Measurement

Gas permeation was studied for the developed membranes with single gases CO₂ and CH₄. Table 3 represents the gas permeation results of pristine polymeric membrane MMM0 and ZIF-7 loaded MMM-20, 30 and 40% membranes. Membranes with higher loading of 50% ZIF-7(MMM50) were brittle and they were not used for gas permeation measurement. An increase of ZIF-7 loading leads to an increase of gas selectivity of CO₂ over CH₄ with a decrease in CO₂ permeability. A similar trend was observed by Li et al., 2010 work on ZIF-7 with Pebax1657.

Table 3. Particle loading in mixed matrix membranes and selectivity towards CO₂/CH₄

Membranes	ZIF-7 loading in wt. (%)	Thickness (μm)	Permeance CO ₂ ($\text{m}^3/\text{m}^2\text{h}\cdot\text{bar}$)	Permeability (Barrer)	Selectivity, α (CO ₂ /CH ₄)
MMM0	N/A	1.5	7.80E-02	43	19
MMM20	19.5	1.9	2.40E-02	16	32
MMM30	23.1	3.5	1.13E-02	14	36
MMM40	33.4	7.3	4.51E-03	13	39

Note: 1Barrer= 10^{-10} cm³ (STP) cm / (cm² s cm Hg).

Feed Pressure: 1 bar, Thickness of membranes were measured from SEM cross-section.

Gas permeance and selectivity of measured samples are summarized in Table 3. The increase of loadings from 20, 30 and 40 wt% caused a decrease of CO₂ permeance whereas the selectivity increased to 68%, 89%, and 99% higher for MMM20, MMM30 and MMM40 compared with the pristine polymeric membrane (MMM0).

4. Conclusions

In summary, we report a series of MMMs with ZIF-7 particles as fillers and PAN-*r*-PEGMA67 polymer for CO₂/CH₄ separation. Structure and morphology of synthesized ZIF-7 particles and developed MMMs were characterized by XRD, FESEM, TEM, FTIR and TGA analysis. Defect-free MMMs were fabricated with 20, 30 and 40 wt% of ZIF-7 loadings. The ZIF particles had a good adhesion with the polymer matrix and no agglomeration was observed. All MMMs, except the brittle MMM50, were measured by constant volume/variable pressure method to evaluate their gas permeance and selectivity with single gases CO₂ and CH₄. MMM with 40% ZIF-7 loading achieved a high selectivity of 39 for CO₂/CH₄ and a CO₂ permeance of 4.51E-03 m³/m²hbar. The increase of ZIF-7 loading in the MMM leads to a small decrease in CO₂ permeance due to the polymer chain rigidification effect.

In conclusion, the resulted ZIF-7/ PAN-*r*-PEGMA67 MMMs showed promising performance for CO₂/CH₄ separation and further works will be continued to enhance the permeance along with selectivity of MMMs for CO₂ separation.

Acknowledgements

We gratefully acknowledge the financial support from King Abdullah University of Science and Technology (KAUST). Authors are thankful to Mahendra Kumar, KAUST – Advanced Membranes & Porous Materials Center, for the polymer synthesis and Ali Behzad from KAUST - Analytical core lab for SEM analysis.

References

- Adewole, J. K., Ahmad, A. L., Ismail, S., & Leo, C. P. (2013). Current challenges in membrane separation of CO₂ from natural gas: A review, *J. membr. Sci.*, 17, 46-65. <https://doi.org/10.1016/j.ijggc.2013.04.012>
- Ahmad, A. L., Jawad, Z. A., Low, S. C., & Zein, S. H. S. (2014). A cellulose acetate/multi-walled carbon nanotube mixed matrix membrane for CO₂/N₂ separation. *Journal of Membrane Science*, 451, 55-66. <https://doi.org/10.1016/j.memsci.2013.09.043>

- Alaslai, N., Ghanem, B., Alghunaimi, F., Litwiller, E., & Pinnau, I. (2016). Pure-and mixed-gas permeation properties of highly selective and plasticization resistant hydroxyl-diamine-based 6FDA polyimides for CO₂/CH₄ separation. *Journal of Membrane Science*, 505, 100-107. <https://doi.org/10.1016/j.memsci.2015.12.053>
- Al-Maythaly, B. A., Alloush, A. M., Faizan, M., Dafallah, H., Elgzoly, M. A., Seliman, A. A., ... & Yaghi, O. M. (2017). Tuning the interplay between selectivity and permeability of ZIF-7 mixed matrix membranes. *ACS applied materials & interfaces*, 9(39), 33401-33407. <https://doi.org/10.1021/acsami.6b15803>
- Bae, T. H., Lee, J. S., Qiu, W., Koros, W. J., Jones, C. W., & Nair, S. (2010). A high-performance gas-separation membrane containing submicrometer-sized metal-organic framework crystals. *Angewandte Chemie International Edition*, 49(51), 9863-9866. <https://doi.org/10.1002/anie.201006141>
- Baker, R. W. (2001). Future directions of membrane gas-separation technology. *Membr. Technol.*, 138, 5-10. [https://doi.org/10.1016/S0958-2118\(01\)80332-3](https://doi.org/10.1016/S0958-2118(01)80332-3)
- Baker, R., & Lokhandwala, K. (2008). Natural Gas Processing with Membranes: An Overview. *Ind. Eng. Chem. Res.*, 47, 2109-2121. <https://doi.org/10.1021/ie071083w>
- Bhide, B. D., & Stern, S. A. (1993). Membrane processes for the removal of acid gases from natural gas. I. Process configurations and optimization of operating conditions. *J. membr. Sci.*, 81, 209-237. [https://doi.org/10.1016/0376-7388\(93\)85175-V](https://doi.org/10.1016/0376-7388(93)85175-V)
- Bottoms, R. R. (Girdler Corp.). (1930). Separating acid gases. *U.S. Patent 1783901*.
- Car, A., Stropnik, C., Yave, W., & Peinemann K. V. (2008). PEG modified poly (amide-b-ethylene oxide) membranes for CO₂ separation, *J. membr. Sci.*, 307, 88-95. <https://doi.org/10.1016/j.memsci.2007.09.023>
- Dai, Y., Johnson, J. R., Karvan, O., Sholl, & Koros, W. J. (2012). Ultem®/ZIF-8 mixed matrix hollow fiber membranes for CO₂/N₂ separations, *J. membr. Sci.*, 401, 76-82. <https://doi.org/10.1016/j.memsci.2012.01.044>
- Kang, C. H., Lin, Y. F., Huang, Y. S., Tung, K. L., Chang, K. S., Chen, J. T., Hung, W. S., Lee K. R., & Lai, J. Y. (2013). Synthesis of ZIF-7/chitosan mixed-matrix membranes with improved separation performance of water/ethanol mixtures, *J. membr. Sci.*, 438, 105-111. <https://doi.org/10.1016/j.memsci.2013.03.028>
- Karunakaran, M., Kumar, M., Shevate, R., Akhtar, F. H., & Peinemann, K-V. (2017). CO₂-Philic thin film composite membranes: synthesis and characterization of PAN-r-PEGMA copolymer, *Polymers*, 9, 219-234. <https://doi.org/10.3390/polym9070219>
- Li, T., Pan, Y., Peinemann, K. V., & Lai, Z. (2013) Carbon dioxide selective mixed matrix composite membrane containing ZIF-7 nano-fillers. *J. membr. Sci.*, 425, 235-242. <https://doi.org/10.1016/j.memsci.2012.09.006>
- Li, Y. S., Liang, F. Y., Bux, H., Feldhoff, A., Yang, W. S., & Caro, J. (2010). Molecular sieve membrane: supported metal-organic framework with high hydrogen selectivity, *Angew. Chem.*, 122, 558-561. <https://doi.org/10.1002/anie.200905645>
- Park, K. S., Ni, Z., Côté, A. P., Choi, J. Y., Huang, R., Uribe-Romo, F. J., ... & Yaghi, O. M. (2006). Exceptional chemical and thermal stability of zeolitic imidazolate frameworks. *Proceedings of the National Academy of Sciences*, 103(27), 10186-10191. <https://doi.org/10.1073/pnas.0602439103>
- Parker, P. M. E., Northrop, S., Valencia, J. A., Foglesong, R. E., & Duncan, W. T. (2011). CO₂ management at ExxonMobil's LaBarge field, Wyoming, USA. *Energy Procedia*, 4, 5455-5470.
- Robeson, L. M. (2008). The upper bound revisited. *J. membr. Sci.*, 320, 390-400.
- Rochell, G. T. (2009). Amine scrubbing for CO₂ capture, *Science*, 325, 1652-1654. <https://doi.org/10.1126/science.1176731>
- Rodenas, T., Luz, I., Prieto, G., Seoane, B., Miro, H., Corma, A., Kapteijn, F., Xamena, F. X. L. I., & Gascon, J. (2015). Metal-organic framework nanosheets in polymer composite materials for gas separation, *Nat. Mater.*, 14, 48-55. <https://doi.org/10.1038/nmat4113>
- Schell, W. J., Wensley, C. G., Chen, M. S. K., Venugopal, K. G., Miller, B. D., & Stuart, J. A. (1989). Recent advances in cellulosic membranes for gas separation an pervaporation, *Gas. Sep. Purif*, 3, 162-169. [https://doi.org/10.1016/0950-4214\(89\)80001-5](https://doi.org/10.1016/0950-4214(89)80001-5)

- Song, Q., Nataraj, S. K., Roussenova, M. V., Tan, J. C., Hughes, D. J., Li, W., ... & Sivaniah, E. (2012). Zeolitic imidazolate framework (ZIF-8) based polymer nanocomposite membranes for gas separation. *Energy & Environmental Science*, 5(8), 8359-8369. <https://doi.org/10.1039/C2EE21996D>
- Tu, M., Wiktor, C., Roßler, C., & Fischer, R. A. (2014). Rapid room temperature syntheses of zeolitic-imidazolate framework (ZIF) nanocrystals, *Chem. Commun.*, 50, 13258-13260. <https://doi.org/10.1039/C4CC06491G>
- van den Bergh, J., Gücüyener, C., Pidko, E. A., Hensen, E. J., Gascon, J., & Kapteijn, F. (2011). Understanding the Anomalous Alkane Selectivity of ZIF-7 in the Separation of Light Alkane/Alkene Mixtures. *Chemistry-A European Journal*, 17(32), 8832-8840. <https://doi.org/10.1002/chem.201100958>
- Wang, X., Chen, J., Fang, M., Wang, T., Yu, L., & Li, J. (2016). ZIF-7/PDMS mixed matrix membranes for pervaporation recovery of butanol from aqueous solution, *Sep. Purif. Technol.*, 163, 39-47. <https://doi.org/10.1016/j.seppur.2016.02.040>
- Xiaochun, H., Jiepeng, Z., & Xiaoming, C. (2003). [Zn(bim)₂](H₂O)1.67: A metal-organic open-framework with sodalite topology, *Chin. Sci. Bull.*, 48, 1531-1534. <https://doi.org/10.1360/03wb0079>
- Zhang, C., Dai, Y., Johnson, J. R., Karvan, O., & Koros, W. J. (2012). High-performance ZIF-8/6FDA-DAM mixed matrix membrane for propylene/propane separations, *J. membr. Sci.*, 389, 34-42. <https://doi.org/10.1016/j.memsci.2011.10.003>
- Zhang, Y., Sunarso, J., Liu, S., & Wang, R. (2013). Current status and development of membranes for CO₂/CH₄ separation: A review *Int. J. Greenhouse Gas Control.*, 12, 84-107. <https://doi.org/10.1016/j.ijggc.2012.10.009>

Appendix

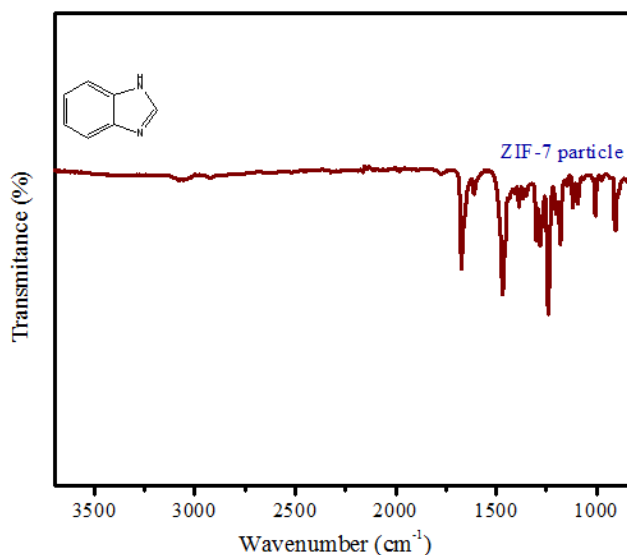


Figure S1. FTIR spectra for ZIF-7 nanoparticles

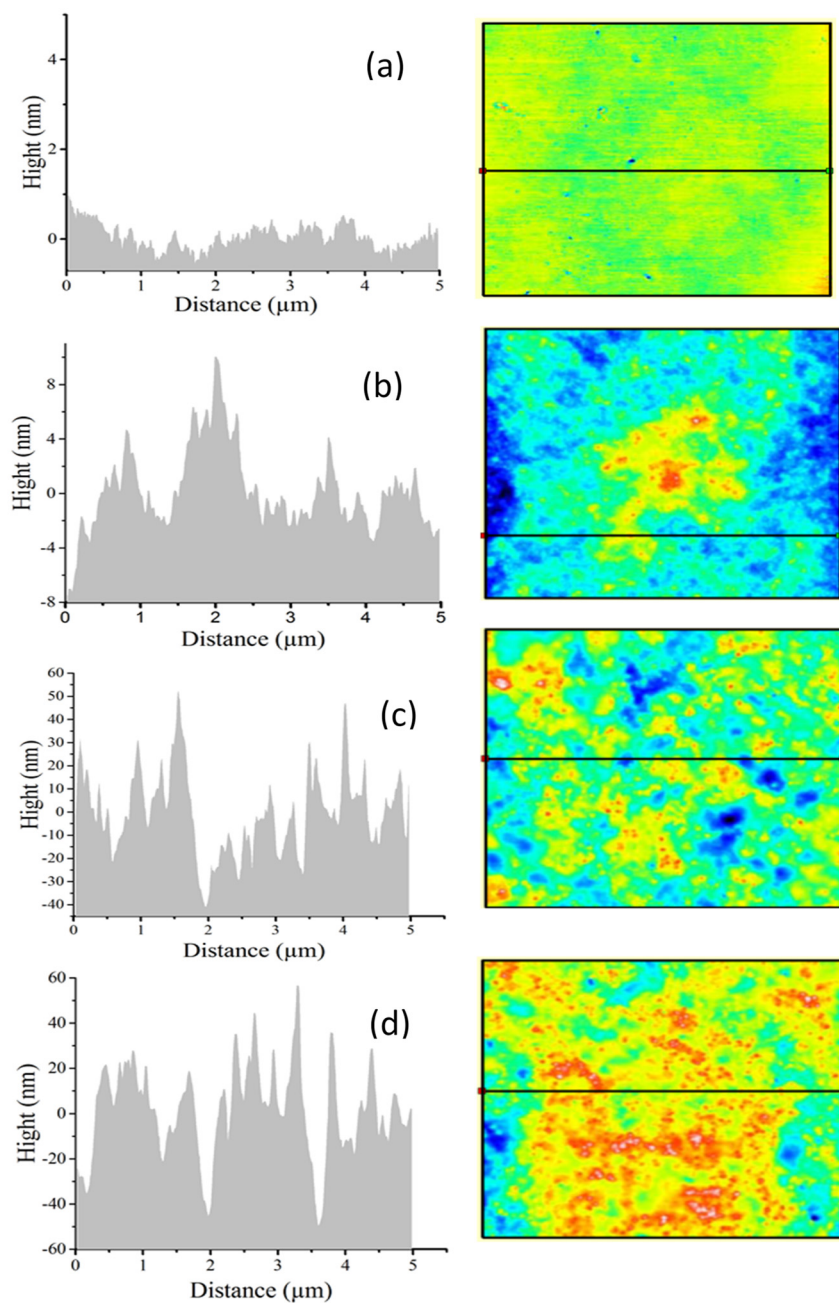


Figure S2 AFM height profile analysis for membranes (a) MMM0 (b) MMM20 (c) MMM30 and (d) MMM40

Copyrights

Copyright for this article is retained by the author(s), with first publication rights granted to the journal.

This is an open-access article distributed under the terms and conditions of the Creative Commons Attribution license (<http://creativecommons.org/licenses/by/4.0/>).